A COMPARISON OF FEATURE EXTRACTION METHODS WITHIN A SPATIO-TEMPORAL LAND COVER CHANGE DETECTION FRAMEWORK

†*W. Kleynhans,, †*B.P. Salmon, †J.C. Olivier, *K.J. Wessels, *F. van den Bergh

† Electrical, Electronic and Computer Engineering University of Pretoria, South Africa

*Remote Sensing Research Unit Meraka Institute, CSIR, Pretoria, South Africa

ABSTRACT

In this paper, a change detection accuracy comparison is made between a recently proposed EKF method and a sliding window Fast Fourier Transform (FFT) alternative within a spatio-temporal change detection framework. Both methods produce a mean and amplitude parameter sequence which is then used to determine a change metric which yield a change of no-change decision after thresholding. The objective is to determine which of these methods produces a change metric value that is able to best discriminate between change and no-change.

1. INTRODUCTION

Anthropogenic land cover change has a major impact on hydrology, climate and ecology [1]. Remote sensing satellite data provide researchers with an effective way to monitor and evaluate land cover changes. Automated change detection reduces human interaction and enables large datasets to potentially be processed in a fraction of the time. Recently, a spatio-temporal framework was proposed for land cover change detection using hyper temporal NDVI time series data. The method models the NDVI time series as a triply modulated cosine function and uses an Extended Kalman filter to estimate the mean and amplitude of the function for each time step. The resulting mean and amplitude parameter sequence of any given pixel is compared to that of its neighboring pixels to infer a change metric. Comparing this change metric with a threshold value yields a change or no-change decision [2].

The objective of this paper is to compare the EKF derived parameter sequence with a sliding window Fast Fourier Transform (FFT) alternative [3] within the afore mentioned spatio-temporal change detection framework. When considering the sliding window FFT approach in the context of the aforementioned spatio-temporal change detection framework. The underlying idea is that a sliding window FFT is computed for the entire time series and that the mean and annual FFT component (i.e FFT component 0 and FFT component 1 when considering a 1 year window) for each time-slice is recorded to produce a resultant mean and amplitude parameter stream. The EKF derived parameter sequence is thus replaced with a sliding window FFT derived mean and amplitude parameter sequence.

Settlement expansion is the most pervasive form of land cover change in South Africa. In particular, the Gauteng province has seen significant new developments being formed from 2001 to 2008. Both algorithms were run in the Gauteng province of South Africa and preliminary results shows that the EKF derived parameter sequence performs better than that of the sliding window FFT when considering the ROC of both methods.

2. METHODOLOGY

2.1. EKF method

The NDVI time series for a given pixel was modeled by a triply modulated cosine function given as

$$y_k = \mu_k + \alpha_k \cos(\omega k + \phi_k) + v_k, \tag{1}$$

where y_k denotes the observed value of the NDVI time series at time k and v_k is the noise sample at time k. The values of μ_k, α_k and ϕ_k are functions of time, and must be estimated given y_k for $k \in 1, \ldots, N$ [4]. An EKF was used to estimate these parameters for every increment of k. The estimated values for $\mathbf{x}_k = [\mu_k \ \alpha_k \ \phi_k]^T$ over time k effectively results in a time series for each of the three parameters.

2.2. Sliding window FFT Method

The Fourier analysis of the NDVI time series is insightful because the signal can be decomposed into a series of cosine waves with varying amplitude, phase and frequency. When considering a window of length w, the discrete Fourier transform of the i'th NDVI time-slice can be written in matrix form as:

$$\mathbf{Y_i} = \mathbf{F}_N \mathbf{y}_i, \tag{2}$$

where $\mathbf{y}_i^T = [y_i \ y_{i+1} \ y_{i+2} \ \ldots \ y_{i+w-1}]$ is the NDVI time series of length w in vector form, $\mathbf{Y_i}^T$ is the FT of $\mathbf{y_i}$ and $\mathbf{F}_w$ is the

DFT matrix in the form

$$\mathbf{F}_w(r,c) = \left[\frac{1}{\sqrt{w}}\, e^{\frac{-2\pi i}{w}}\right]^{(r-1)\cdot(c-1)}, \qquad (3)$$

where $\mathbf{F}_w(r,c)$ is the value of row r and column c of the $\mathbf{F}_w$ matrix. Relating this to the aforementioned EKF method yields

$$\begin{bmatrix} \mu_k \\ \alpha_k \\ \phi_k \end{bmatrix} = \begin{bmatrix} Y_k(1) \\ |Y_k(Y)| \\ \angle Y_k(Y)] \end{bmatrix} \quad k \in \{1, 2, .., N-w+1\},$$

where Y is the number of annual cycles captured in the window size, i.e. if there are 46 samples every year, a window length of 92 will correspond to $Y = 2$.

2.3. Change Detection Method

Having the parameter sequence $\mathbf{x}$ for a given pixel, a change detection method was formulated by comparing the parameter sequences of the pixel with that of its direct neighboring pixels. This effectively means focusing on the center pixel of a 3×3 grid of pixels and examining each neighboring pixel's parameter sequence relative to the center pixel. It was previously established that the ϕ parameter sequence does not yield any significant separability between natural vegetation and settlement land cover types and consequently only the μ and α parameter sequence was considered [4]. The μ and α parameter sequence difference between the center pixel and an arbitrary neighboring pixel at time k can be written as

$$D^k_{\mu(n)} = |\mu_k - \mu^n_k| \qquad n \in 1, \ldots, 8, \qquad (4)$$

$$D^k_{\alpha(n)} = |\alpha_k - \alpha^n_k| \qquad n \in 1, \ldots, 8, \qquad (5)$$

where $D^k_{\mu(n)}$ is the distance between the μ parameter sequence of a selected pixel (μ_k) with its n'th neighboring pixel (μ^n_k) at time k. $D^k_{\alpha(n)}$ is the distance between the α parameter streams of a selected pixel (α_k) with its n'th neighboring pixel (α^n_k) at time k. Equation 4 and 5 can be combined as

$$D^k_n = D^k_{\mu(n)} + D^k_{\alpha(n)} \qquad n \in 1, \ldots, 8. \qquad (6)$$

Having obtained a distance relative to each of the neighboring pixels, these could be combined at time k by simply adding all the values of D^k_n $n \in 1, \ldots, 8$ at time k

$$D^k = \sum_{n=1}^{8} D^k_n \qquad k \in 1, \ldots, N. \qquad (7)$$

Having vector $\mathbf{D} = [D^1\ D^2\ D^3\ \ldots\ D^N]$, a change metric was derived by firstly determining how the relative distance between the center pixel and its neighboring pixel changes through time. This was done by differentiating the vector D. A single change metric was then derived by summing all the values of the differentiated D vector to yield

$$\delta = \sum_{k=2}^{N} |D^k - D^{k-1}|, \qquad (8)$$

where δ is a single valued change metric for the center pixel of the 3x3 pixel grid. The change metric for each of the pixels in the study area was thus calculated by sliding a 3x3 pixel grid over the entire study area and calculating δ for the center pixel.

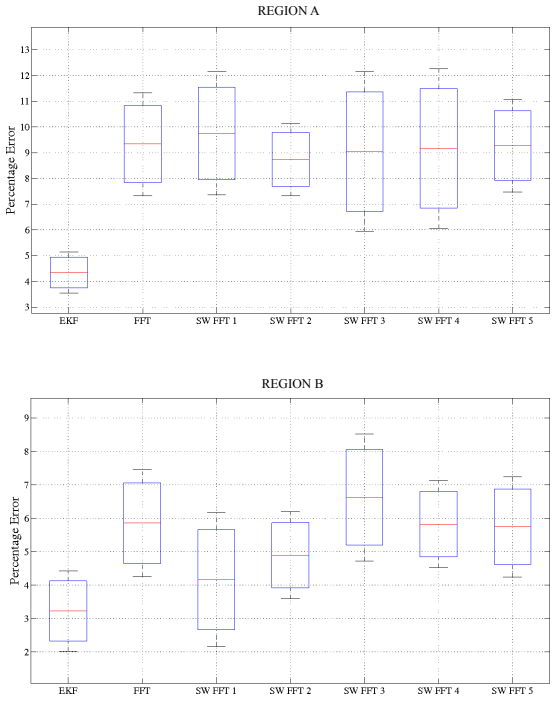

Fig. 1. The Bayes' error and variance for the EKF and SW FFT method for region A and B. The window size of the SW FFT method was varied between one and five years.

3. RESULTS

3.1. Separability Results

As an initial experiment, the land cover class separability between natural vegetation and settlement land cover types were evaluated using the features obtained using each of the discussed methods. The underlying idea is that the separability of the features (obtained using the sliding window FFT and EKF method respectively) would be indicative of the eventual land cover change detection accuracy.

The proposed methods were tested in two regions in South Africa. The first study area (Region A) is centered around lat-

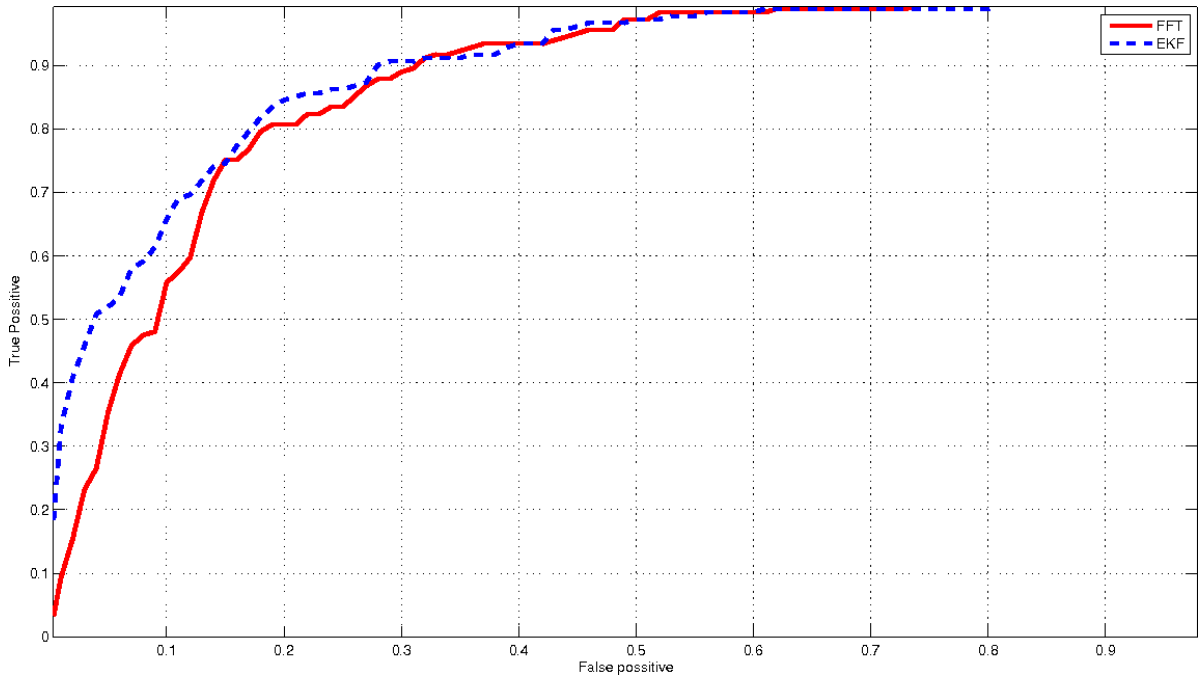

Fig. 2. Receiver operating characteristic for the sliding window FFT (1 year sliding window) and EKF approach.

itude $24°17'21.43''$S and longitude $29°39'42.96''$E and is 43 km south east of the city of Polokwane. Region A covers a geographic area of approximately 190 km^2, 42 natural vegetation and 42 settlement pixels were selected for analysis.
Region B is centered around latitude $24°19'51.50''$S and longitude $29°18'04.07''$E and is 47 km south west of the city of Polokwane. Region B covers a geographical area of 100 km^2, 32 settlement and 61 natural vegetation pixels were selected. The study regions that were considered had settlements and natural vegetation areas in close proximity which ensured that the rainfall, soil type and local climate were similar.

The Bayes error was calculated and used to determine the performance of each method. The underlying idea is that the lower the Bayes error, the more "unique" the distributions and consequently, the better the class separability. The Bayes' error for the EKF and sliding window (SW) FFT method together with the corresponding variance of each of these methods are shown in figure 1 . The window size of the SW FFT method was varied between one and five years, denoted as SW FFT 1 to SW FFT 5. The full window, which contains the complete time-series is also given for comparison and is denoted as FFT (figure 1).

3.2. Change detection results

The change detection performance was evaluated in the Gauteng province which is located in northern South Africa. Because of a high level of urbanization it has seen significant human settlement expansion during the 2001 and 2008 period. A total area of approximately 17 000 km^2 was considered being centered around $26°07'29.62''$S, $28°05'40.40''$E. Gauteng is the smallest province in South Africa, occupying a land area of only 1.4% of the land area of the country, but it is highly urbanized as it contains two of the largest cities in South Africa, Johannesburg and Pretoria. A total of 592 examples of natural vegetation, 372 examples of settlement and 181 examples of real change 500 m MODIS pixels were identified within the study area. Landsat and SPOT high resolution data were used to identify the aforementioned pixels.

The Receiver Operator Characteristic (ROC) , which considered the change detection accuracy (true positive) as a function of the false alarm rate (false positive) is shown for both methods in the study area (figure 2). It can be seen that, for example, at a false alarm rate of 10%, there is almost a 10% difference in the change detection accuracy as the EKF method has a change detection accuracy of 67% where the SW FFT method has a change detection accuracy of 57%.

4. CONCLUSION

In this paper, a spatio-temporal approach using both an EKF and sliding window FFT approach was evaluated. As an initial experiment, the land cover separability that was achievable using the features obtained using both methods where considered. It found that the EKF method provided better sep-

arability when compared to the sliding window FFT method, regardless of the window size. This result was confirmed when the change detection performance of both methods were considered in the Gauteng province of South Africa. The ROC of both methods showed that, although both methods performed well overall, the EKF approach provided a definite advantage when considering a false alarm rate in the region between zero and 15% (figure 2).

5. REFERENCES

[1] R. T. Watson, *Land Use, Land-Use Change and Forestry*, Cambridge University Press, Cambridge, England, 2000.

[2] W. Kleynhans, J. C. Olivier, K. J. Wessels, B. P. Salmon, F. van den Bergh, and K. Steenkamp, "Detecting land cover change using an extended kalman filter on modis ndvi time-series data," *IEEE Geoscience and Remote Sensing Letters*, vol. 8, no. 3, pp. 507–511, May 2011.

[3] B. P. Salmon, J. C. Olivier, K. J. Wessels, W. Kleynhans, F. van den Bergh, and K. Steenkamp, "Automated land cover change detection using MODIS satellite time series data: Introducing the temporal sliding window," *IEEE Transactions of Automated Science and Engineering*.

[4] W. Kleynhans, J. C. Olivier, K. J. Wessels, B. P. Salmon, F. van den Bergh, and K. Steenkamp, "Improving land cover class separation using an extended Kalman filter on MODIS NDVI time series data," *IEEE Geoscience and Remote Sensing Letters*, vol. 7, no. 2, pp. 381–385, Apr. 2010.